Monte Carlo study of liquid ^{3}He-^{4}He solutions

Wing-Kee Lee* and Bernard Goodman
Department of Physics, University of Cincinnati, Cincinnati, Ohio 45221
(Received 24 November 1980)

The ground state of liquid ^{3}He-^{4}He solution was represented by a Jastrow wave function times Slater determinants for the ^{3}He atoms, and a Monte Carlo calculation was performed for ^{3}He concentrations of 6.5, 12, and 44 at.%. The average binding energy per atom, the radial distribution functions, the structure functions, the momentum distribution of the ^{4}He atoms, and the ^{4}He condensate fraction n_0 were calculated. In the above concentrations, the values of n_0 were found to be $13.1 \pm 1\%$, $13.7 \pm 1\%$, and $19.0 \pm 1\%$, respectively, compared to 11% for bulk liquid ^{4}He. This enhancement of n_0 is due mainly to the decreasing density of the solution as the ^{3}He concentration increases. Similar calculations were done for mass-3–mass-4 boson solutions. The radial distribution function of the ^{3}He-^{4}He solution are different from those of the mass-3–mass-4 boson solutions due to the difference in statistics.

I. INTRODUCTION

The static properties of liquid ^{3}He-^{4}He solutions in the limit of zero ^{3}He concentration have been calculated by many researchers.[1] The calculated values of the binding energy of ^{3}He atoms to the ^{4}He medium is in agreement with experiment and, until very recently,[2] this was considered to be the case also for the effective mass of ^{3}He quasiparticles. On the other hand, static properties like the radial distribution functions and the condensate fraction have not been calculated for finite ^{3}He concentrations. Here we report a calculation of the ground-state radial distribution functions and the condensate fraction n_0 of the ^{4}He atoms in liquid ^{3}He-^{4}He solutions with ^{3}He concentrations x equal 6.5, 12, and 44 at.%.

The theory of condensate fraction of pure liquid ^{4}He was advanced by Penrose and Onsager[3] who have shown that n_0 can be deduced from the asymptotic value of the single-particle density matrix $\rho_1^4(r)$ at large r. They estimated for n_0 a value of 8%. All the calculations listed below, except that of Whitlock *et al.*,[9] make use of the idea of Penrose and Onsager and represent liquid ^{4}He by the Jastrow wave function.

$$\psi(\vec{r}_1, \ldots, \vec{r}_N) = \exp\left[-\frac{1}{2}\sum_{i<j}^{N} u(r_{ij})\right] , \qquad (1)$$

where N is the number of ^{4}He atoms and $u(r)$ is an optimized function. The Monte Carlo calculations of McMillan,[4] the molecular dynamics calculation of Schiff and Verlet,[5] and the integral equation method of Francis *et al.*[6] all give a n_0 of about 11% at 0 K. McMillan calculated n_0 for the zero-pressure equilibrium density while Schiff and Verlet calculated it as a function of density for densities higher than the equilibrium value. The result of Francis *et al.* indicates that the zero-point phonons lower the condensate fraction by 2%. On the other hand, Lam and Chang[7] did a calculation using a diagrammatic cluster approach which indicates that an optimized Jastrow correlation function $u(r)$ of Eq. (1) with an intermediate and long-range structure gives a larger n_0 than short range $u(r)$ alone, in conflict with the findings of Francis *et al.* Lam and Chang also found that n_0 is sensitive to the potential used. Reatto has shown generally that calculations using Jastrow wave functions should give a nonzero condensate fraction.[8] The calculation of Whitlock *et al.*[9] which solves the Schrödinger equation for hard spheres numerically by a Green's-function Monte Carlo method gives a condensate fraction of about 11%. A more complete list of references on the condensate fraction and its relation to superfluidity is given in the review article of Chester.[10]

It was suggested by Hohenberg and Platzman[11] that the condensate fraction of liquid ^{4}He can be deduced from the dynamic structure factor $S(Q, \omega)$ of inelastic neutron scattering at high momentum transfer Q. The analyses of neutron scattering data by Mook *et al.*, Rodriguez *et al.*, Mook, and Aleksandrov *et al.*[12] all give a condensate fraction of about 2% at about 1.1 K. The analyses of neutron scattering data by Harling[13] and Woods and Sears[14] give larger values of the condensate fraction, namely, 8.8% (at 1.27 K) and 6.9% (at 1.1 K), respectively. Dokukin *et al.*[15] have measured the condensate fraction as function of temperature $n_0(T)$ by using neutron scattering and fit their data to

$$n_0(T) = n_0(0)[1 - (T/T_\lambda)^m] , \qquad (2)$$

where $n_0(0) = 0.024 \pm 0.004$, $T_\lambda = 2.29 \pm 0.12$ K, and $m = 5.6 \pm 4$. All the above-mentioned experiments are based on the idea of Hohenberg and Platzman.

On the other hand, the most recent experimental analysis of Sears and Svensson,[16] which is based on the static radial distribution function,[17,18] inferred values for $n_0(0)$ and m in Eq. (2) of 0.133 ± 0.012 and 6.2 ± 1.6, respectively.

The present calculations for ^{3}He-^{4}He solutions are based on the Slater-Jastrow wave function which represents the ground state and therefore zero temperature. The multidimensional integrals are performed by using the Monte Carlo method of McMillan[4] as extended to fermions by Ceperley *et al.*[19] For real solutions phase separation occurs for $x > 6.5\%$ at 0 K.[20] However, in our Monte Carlo simulation we found no evidence of phase separation in the study of the spatial distribution of the ^{3}He and ^{4}He atoms even for considerably larger values of x. This is presumably due to the fact that our runs are too short to simulate phase separation. Furthermore, the small number of particles (at most 38 ^{3}He atoms and 49 ^{4}He atoms) in the period cell and the use of periodic boundary conditions probably also inhibit phase separation. As will be discussed later, some features of the zero-temperature calculation should still be relevant for nonzero temperatures at which the real solutions with the above ^{3}He concentrations are stable.

II. METHOD OF CALCULATION

The Hamiltonian of the solution is

$$H = -\frac{\hbar^2}{2m_3}\sum_{i=1}^{N_3}\nabla_i^2 - \frac{\hbar^2}{2m_4}\sum_{i=N_3+1}^{N=N_3+N_4}\nabla_i^2 + \sum_{i<j}^{N} V(r_{ij}) \ ,$$

where N_3 and N_4 are the number of ^{3}He and ^{4}He atoms, respectively, and $V(r)$ is taken to be the Lennard-Jones potential

$$V(r) = 4\epsilon\left[\left(\frac{\sigma}{r}\right)^{12} - \left(\frac{\sigma}{r}\right)^{6}\right] \ ,$$

with $\epsilon = 10.22$ K and $\sigma = 2.556$ Å.

The ground state of the solution is described by a Slater-Jastrow wave function,

$$\psi(\vec{r}_1, \ldots, \vec{r}_{N_3}; \vec{r}_{N_3+1}, \ldots, \vec{r}_N) = \exp\left[-\frac{1}{2}\sum_{i<j\le N_3} u^{(3,3)}(r_{ij}) - \frac{1}{2}\sum_{\substack{N_3+1\le j\le N \\ i\le N_3}} u^{(3,4)}(r_{ij}) - \frac{1}{2}\sum_{N_3+1\le i\le j\le N} u^{(4,4)}(r_{ij})\right] d_\uparrow d_\downarrow \ , \quad (3)$$

where $d_\uparrow$ and $d_\downarrow$ are Slater determinants for up-spin ^{3}He and down-spin ^{3}He atoms, respectively. The orbitals used in the determinants are $\cos[(2\pi/L)\times(\vec{n}\cdot\vec{x})]$ and $\sin[(2\pi/L)(\vec{n}\cdot\vec{x})]$, where $\vec{n}$ are integer vectors satisfying $2\pi|\vec{n}|/L < k_F$, k_F being the Fermi momentum of the ^{3}He atoms and L is the size of the cubic period cell.

For a given ^{3}He fraction, x, L is determined by the relation

$$L^3 = N v_4(1+\alpha x) \ , \quad (4)$$

where $v_4 = 2.75\sigma^3$ is the measured volume per atom in liquid ^{4}He at its 0-K equilibrium density, and α, the excess volume fraction, is taken to be 0.284 as measured by Edwards *et al.*[21] Appropriate numbers of ^{3}He and ^{4}He atoms are put into this box to give the desired concentration, and periodic boundary conditions are used. The number of ^{3}He atoms are chosen such that the Fermi sphere is occupied cubically symmetrically for each spin orientation. The Jastrow factors are all chosen to be the same,

$$u^{(3,3)}(r) = u^{(3,4)}(r) = u^{(4,4)}(r) \equiv u(r) = (b\sigma/r)^5 \ , \quad (5)$$

where b is a variational parameter. This form of $u(r)$ has been extensively used for pure ^{4}He and pure ^{3}He calculations.[4,5,19]

The expectation value (per atom) of the Hamiltonian which is obtained by direct differentiation of ψ, can be written as

$$E = x(T_3 + V_3) + (1-x)(T_4 + V_4) \ , \quad (6)$$

where

$$\begin{aligned}
V_\alpha &= \frac{1}{N_\alpha}\left\langle \frac{1}{2}\sum_l \sum_j{}' V(r_{lj})\right\rangle \ , \\
T_\alpha &= 2T'_\alpha - F_\alpha^2 \ , \\
T'_\alpha &= T_{u\alpha} + \tfrac{1}{2}\delta_{\alpha 3}(K_D + F_D^2) \ , \\
T_{u\alpha} &= \frac{1}{8m_\alpha N_\alpha}\left\langle \sum_l \sum_j{}' \nabla_l^2 u(r_{lj})\right\rangle \ , \quad (7) \\
K_D &= -\frac{\hbar^2}{2m_3 N_3}\left\langle \sum_{l=1}^{N_3}\sum_{k=1}^{N_\uparrow} \bar{D}^s_{kl}\nabla_l^2\phi_k(\vec{r}_l)\right\rangle \ , \\
F_D^2 &= \frac{\hbar^2}{2m_3 n_3}\left\langle \sum_{l=1}^{N_3}\left[\sum_{k=1}^{N_\uparrow}\bar{D}^s_{kl}\nabla_l\phi_k(\vec{r}_l)\right]^2\right\rangle \ , \\
F_\alpha^2 &= \frac{\hbar^2}{2m_\alpha N_\alpha}\left\langle \sum_l\left[\frac{1}{2}\sum_j{}'\nabla_l u(r_{lj}) - \delta_{\alpha 3}\sum_{k=1}^{N_\uparrow}\bar{D}^s_{kl}\nabla_l\phi_k(\vec{r}_l)\right]^2\right\rangle \ ,
\end{aligned}$$

$\alpha = 3$ or 4 .

The sum $\sum_l$ is taken over the α species *only*, while the sum $\sum_j'$ is over *all* the j's not equal to l. Here $\phi_k(\vec{r}_l)$ are the occupied orbitals in the Slater determinants and the superscript s denotes the spin state ($\uparrow$ or $\downarrow$). $\bar{D}^s_{kl}$ are the elements of the inverse of the transpose of the matrix of d_s whose elements are $D^s_{kl}=\phi_k(\vec{r}_l)$; that is,

$$\sum_{l=1}^{N_\uparrow}\bar{D}^s_{il}D^s_{kl}=\delta_{ik} \ .$$

The dimension of each of these matrices is $N_\uparrow = N_3/2$. We note here that the first subscript of $\bar{D}^s_{kl}$ is the label of an orbital while the second subscript is the label of a ^{3}He atom. In Eq. (7), $\langle f \rangle$ is the expectation value

$$\int f\psi^2\, d^3r_1\cdots d^3r_N \Big/ \int \psi^2\, d^3r_1\cdots d^3r_N \ .$$

T_α and V_α are just the average kinetic energy and the average potential energy of a $^\alpha$He atom, respectively. A simple integration by parts gives

$$T'_\alpha = F^2_\alpha \ , \tag{8}$$

and hence $T'_\alpha = T_\alpha = F^2_\alpha$.[22]

By using the explicit form of $\phi_j(r_j)$, namely, $\cos(\vec{k}_j\cdot\vec{r}_i)$ or $\sin(\vec{k}_j\cdot\vec{r}_i)$, K_D can be simplified to

$$K_D=\frac{\hbar^2}{2m_3N_3}\left\langle\sum_{i=1}^{N_3}\sum_{j=1}^{N_\uparrow}\bar{D}^s_{ji}k_j^2\phi_j(\vec{r}_i)\right\rangle=\frac{\hbar^2}{2m_3N_3}\sum_{j=1}^{N_\uparrow}k_j^2 \ , \tag{9}$$

where the property $\sum_i \bar{D}^s_{ji}\phi_j(\vec{r}_i)=1$ has been used. That is, K_D gives the ideal gas kinetic energy per atom, independent of the trial wave function. It is clear that Eq. (9) holds for every configuration not just as an average. Notice that for an *ideal* Fermi gas, which can be described by the wave function ψ in Eq. (3) with all the u's equal to zero, Eq. (8) reduces to

$$K_D = F_D^2 \ . \tag{10}$$

For an interacting fermion system this is no longer true. However, the quantity

$$T_D=\tfrac{1}{2}(K_D+F_D^2) \ , \tag{11}$$

can be identified as the kinetic energy due to the Slater determinants.

The wave function is optimized by a variational calculation similar to that detailed by McMillan.[4] In order to handle the Slater determinants, we have used the procedure developed by Ceperley *et al.*[19] Our Monte Carlo program was coded in FORTRAN and was tested by repeating the pure liquid ^{4}He calculations of McMillan and the pure liquid ^{3}He calculations of Ceperley *et al.* Our results are in good agreement with theirs.

We extract the condensate fraction from the single-particle density matrix of the ^{4}He atoms, which is defined as

$$\rho_1^4(|r-r'|)=N_4\int\psi(\vec{r}_1,\ldots,\vec{r}_{N_3};\vec{r}',\vec{r}_{N_3+2},\ldots,\vec{r}_N)\psi(\vec{r}_1,\ldots,r_{N_3};\vec{r},\vec{r}_{N_3+2},\ldots,\vec{r}_N)$$
$$\times d^3r_1\cdots d^3r_{N_3}d^3r_{N_3+2}\cdots d^3r_N\Big/\int\psi^2\, d^3r_1\cdots d^3r_N \ ,$$

which, using the wave function (3), can be written in the different form

$$\rho_1^4(r)=\rho_4\left\langle\frac{1}{N_4}\sum_{i=N_3+1}^{N}\exp\left[-\tfrac{1}{2}\sum_{j\neq i}^{N}[u(|\vec{r}_i+\vec{r}-\vec{r}_j|)-u(|\vec{r}_i-\vec{r}_j|)]\right]\right\rangle \ , \tag{12}$$

where ρ_4 is the number density of the ^{4}He atoms. $\rho_1^4(r)$ can then be calculated by Monte Carlo method. The condensate fraction of the ^{4}He atoms is given by[3]

$$n_0=\rho_1^4(\infty)/\rho_4 \ .$$

In practice $\rho_1(r)$ becomes constant for $r\gtrsim 2\sigma$.

For the 44% solution we have also calculated the single-particle density matrix of the ^{3}He atoms which is given by

$$\rho_1^3(r)=\rho_3\left\langle\frac{1}{N_3}\sum_{i=1}^{N_3}\left[\exp\left[-\tfrac{1}{2}\sum_{j\neq i}^{N}[u(|\vec{r}_i+\vec{r}-\vec{r}_j|)-u(|\vec{r}_i-\vec{r}_j|)]\right]\right]\sum_{l=1}^{N_\uparrow}\bar{D}^s_{li}\phi_l(\vec{r}+\vec{r}_i)\right\rangle \ . \tag{13}$$

The radial distribution functions are defined as

$$g_{\alpha\beta}(|\vec{x}_1-\vec{x}_2|)=\frac{1}{\rho_\alpha\rho_\beta}\left\langle\sum_{i\alpha}^{N_\alpha}\sum_{j\beta}^{N_\beta}(1-\delta_{i\alpha,j\beta})\delta(\vec{x}_1-\vec{r}_{i\alpha})\delta(\vec{x}_2-\vec{r}_{j\beta})\right\rangle \ , \tag{14}$$

where $\alpha, \beta = 3$ or 4, and ρ_α, ρ_β are the number densities of the α species and the β species, respectively, while $\vec{r}_{i\alpha}$ and $\vec{r}_{j\beta}$ denote the positions of a α atom and a β atom, respectively. We have neglected spin in the above definition. To include the fermion spin, let $\vec{r}_i\sigma_i$ be the space and spin coordinates of a ^{3}He atom. We define the radial distribution function for parallel spins by

$$g_p(x_{12}) = g_p(|\vec{x}_1 - \vec{x}_2|) = \frac{1}{\rho_3^2}\left\langle \sum_{i\neq j}^{N_3} \delta_{\sigma_i\sigma_j}\delta(\vec{x}_1 - \vec{r}_i)\delta(\vec{x}_2 - \vec{r}_j)\right\rangle , \quad (15)$$

and the radial distribution function for antiparallel spins by

$$g_a(x_{12}) = \frac{1}{\rho_3^2}\left\langle \sum_{i,j}^{N_3} (1-\delta_{\sigma_i\sigma_j})\delta(\vec{x}_1 - \vec{r}_i)\delta(\vec{x}_2 - \vec{r}_j)\right\rangle . \quad (16)$$

(Note that g_p and g_a, as defined here, each approach the value $\frac{1}{2}$ at large separation.) It is clear that

$$g_{33}(r) = g_p(r) + g_a(r) .$$

The radial distribution functions $g_{\alpha\beta}(r)$ are calculated by the following procedure[4]: Compute the distance between each α-β pair, and count the number of such distances which lie in a bin between $r - \frac{1}{2}\Delta r$ and $r + \frac{1}{2}\Delta r$. Averaging this number over the configuration gives us an estimate of

$$\begin{cases} \frac{1}{2}N_\alpha\rho_\alpha 4\pi r^2 g_{\alpha\alpha}(r)\Delta r, & \text{if } \alpha = \beta , \\ N_\alpha\rho_\beta 4\pi r^2 g_{\alpha\beta}(r)\Delta r, & \text{if } \alpha \neq \beta . \end{cases} \quad (17)$$

This applies for wave functions with or without Slater determinants. $g_p(r)$ and $g_a(r)$ are calculated by the same procedure.

The structure factors are calculated by Fourier transforming the corresponding radial distribution functions as follows:

$$\begin{aligned} S_{\alpha\beta}(k) &= \delta_{\alpha\beta} + (\rho_\alpha\rho_\beta)^{1/2}\int [g_{\alpha\beta}(r) - 1]e^{i\vec{k}\cdot\vec{r}}\, d^3r , \\ S_p(\vec{k}) &= 1 + \rho_3 \int [g_p(r) - \tfrac{1}{2}]e^{i\vec{k}\cdot\vec{r}}\, d^3r , \\ S_a(\vec{k}) &= \rho_3 \int [g_a(r) - \tfrac{1}{2}]e^{i\vec{k}\cdot\vec{r}}\, d^3r . \end{aligned} \quad (18)$$

Notice that $S_{33}(k) = S_p(k) + S_a(k)$.

III. NUMERICAL RESULTS

For simplicity we will denote a calculation by (N_3, N_4), where N_3 and N_4 are, respectively, the number of ^{3}He and ^{4}He atoms put into the period cell to give the desired concentration.

The functions $g_{\alpha\beta}(r)$, $g_p(r)$, $g_a(r)$, $\rho_1^3(r)$, and $\rho_1^4(r)$ obtained are not smooth because of sampling, and it was considered too expensive to accumulate enough statistics to give essentially smooth curves directly. We have smoothed these functions by using the DSE15 routine of IBM, which smoothes the data points at $x_i (i = 1, \ldots, n)$ by the following procedure: Except at the end points x_1, x_2, x_{n-1}, x_{n-2}, the smoothed value at x_i is obtained by evaluating at x_i the linear least-squares fit to the five points $x_{i-2}, \ldots, x_{i+2}$. This smoothing gets rid of, to large extent, the unreasonable differences of the values of adjacent bins.

A. Solution with 44% ^{3}He concentration

The expectation value of the Hamiltonian per atom, E, obtained from a (14,18) calculation ($x = 43.75\%$, $\rho_3 = 0.141\sigma^{-3}$, and $\rho_4 = 0.182\sigma^{-3}$), is plotted against b in Fig. 1. The optimal value of b is taken to be 1.145 which appears to give the lowest energy. E and the relevant average quantities as functions of b and concentrations are presented in Table I. In Table I, the statistical uncertainties are obtained by the following procedure which is typical for such calculations.[23] Divide a run into $\mathfrak{N}(\approx 7)$ sections containing an equal number of configurations. Compute the quantity of interest by averaging over all the configurations *within each* section and obtain a value, say, A_i for the ith section. The final average is then given by

$$A = \frac{1}{\mathfrak{N}}\sum_{i=1}^{\mathfrak{N}} A_i ,$$

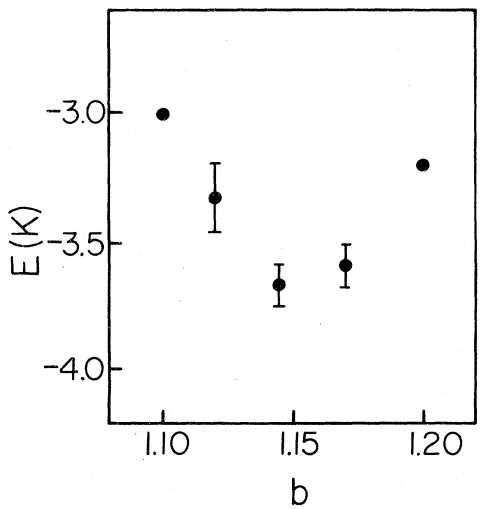

FIG. 1. Expectation value of the Hamiltonian per atom of the 44% solution as a function of b.

TABLE I. Results of the ^{3}He-^{4}He solution calculations. The unit of energy is K/atom.

No.	N_3	N_4	x (%)	b	n (10^3)	E	T_3	F_3^2	V_3	T_4	F_4^2	V_4	K_D	F_D^2	n_0 (%)
1	14	18	43.75	1.100	90[a]	−2.95	14.10	13.55	−14.81	9.75	9.73	−14.66	1.95	1.53	21.0
2	14	18	43.75	1.120	150	−3.31	14.81	14.75	−15.63	10.31	10.37	−15.57	1.95	1.40	20.6
						±0.16	±0.17	±0.43	±0.17	±0.10	±0.25	±0.26		±0.11	
3	14	18	43.75	1.145	180	−3.68	15.85	16.04	−16.61	10.82	10.69	−16.74	1.95	1.75	18.0
						±0.07	±0.19	±0.63	±0.19	±0.10	±0.33	±0.26		±0.40	
4	38	49	43.67	1.145	160	−3.63	15.80	15.84	−16.61	11.01	11.15	−16.66	1.84	1.57	19.0
						±0.08	±0.30	±0.73	±0.18	±0.09	±0.46	±0.16		±0.22	
5	14	18	43.75	1.170	150	−3.59	16.54	16.43	−17.34	11.56	11.58	−17.40	1.95	1.40	15.4
						±0.08	±0.12	±0.44	±0.18	±0.14	±0.42	±0.15		±0.15	
6	14	18	43.75	1.200	90[a]	−3.20	17.75	17.56	−17.94	12.46	12.57	−18.03	1.95	1.65	12.7
7	14	100	12.28	1.160	150	−5.25	17.64	17.87	−18.64	12.87	12.85	−18.72	0.88	0.68	13.7
						±0.03	±0.39	±1.02	±0.35	±0.07	±0.43	±0.32		±0.21	
8	14	201	6.51	1.160	150	−5.45	18.11	18.27	−19.29	13.19	13.19	−18.90	0.58	0.41	13.1
						±0.04	±0.84	±2.11	±0.43	±0.50	±0.50	±0.27		±0.19	
9	14	18[b]	43.75	1.145	150	−4.31	14.32	14.58	−16.44	10.80	10.89	−16.54	0.00	0.00	18.0
						±0.06	±0.14	±0.55	±0.22	±0.12	±0.41	±0.27			

[a]The run is too short for computing the uncertainties.

[b]A calculation in which the determinants are deleted from the wave function.

and the uncertainty is then taken to be the standard deviation,

$$\delta A = \left[\frac{1}{\mathfrak{N}-1} \sum_{i=1} (A_i - A)^2 \right]^{1/2} . \tag{19}$$

To study the effect of the size of the period cell, a (38,49) calculation ($x = 43.68\%$) with $b = 1.145$ was performed and the results are also presented in Table I. The agreement between the (14,18) and the (38,49) calculations is good, which suggests that variational calculations for the larger period cell are not necessary. The insensitivity of the results to the size of the cell is in agreement with the results reported in McMillan's work[4] on pure liquid ^{4}He and by Ceperley *et al.*[19] for pure liquid ^{3}He, and can be attributed to the short-range nature of the Jastrow correlation function $u(r)$. The difference of 0.1 K between the values of K_D of the two calculations is, however, significant. We have seen in Eq. (7) that, for *any* trial wave function, K_D should be the kinetic energy per atom of an ideal Fermi gas with $N_\uparrow (= N_3/2)$ atoms of each spin in the period cell. Since $N_\uparrow$ atoms are used to fill the discrete states inside the Fermi sphere, K_D will fluctuate with $N_\uparrow$ about the value for an infinite system, namely,

$$K_D(N_\uparrow = \infty) = \frac{3}{5} \frac{\hbar^2}{2m_3} \left(3\pi^2 \frac{\rho_3}{2} \right)^{2/3} = 1.918 \text{ K} .$$

From Eq. (9) we obtain

$$K_D(N_\uparrow = 7) = \frac{6}{7^{5/3}} (4\pi^2) \left(\frac{\rho_3}{2} \right)^{2/3} = 1.95 \text{ K} ,$$

$$K_D(N_\uparrow = 19) = \frac{30}{19^{5/3}} (4\pi^2) \left(\frac{\rho_3}{2} \right)^{2/3} = 1.84 \text{ K} .$$

The values of K_D in Table I are calculated explicitly in a Monte Carlo run, that is, by evaluating

$$K_D = \sum_{i=1}^{N_\uparrow} \sum_{j}^{N_\uparrow} \bar{D}_{ji}^{s} \nabla_i^2 \phi_j(\vec{r}_i)$$

at the end of each cycle[24] (after each atom has been moved once). The value should agree precisely with the analytical value if $\bar{D}_{ji}^{s}$ are updated correctly. This serves as another test of our Monte Carlo program. The difference between the values of K_D due to the difference of $N_\uparrow$ does not show up in T_3 due to the relatively large uncertainty of 0.3 K in T_3.

We present below the results of the (38,49) calculation with $b = 1.145$. This larger system is chosen for presentation because the size of the period cell of the smaller system is too small to allow the calculation of $g_{\alpha\beta}(r)$ and $\rho_\uparrow^\alpha(r)$ for $r > 2.3\sigma$,[25] while the larger system can be used to calculate the values of these functions up to $r = 3.22\sigma$. The larger-r behavior of these quantities is important in determining the small-k values of the structure functions $S_{\alpha\beta}(k)$ and the momentum distributions $N^\alpha(k)$.

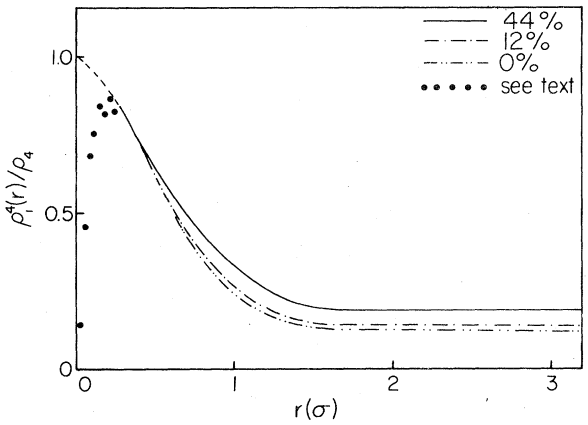

FIG. 2. Single-particle density matrix of the ^{4}He atoms.

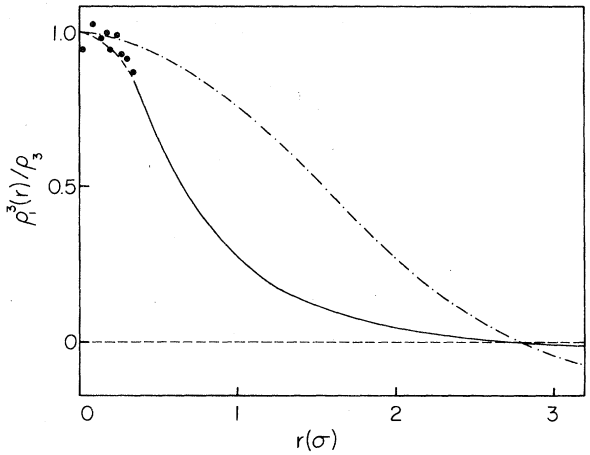

FIG. 3. Single-particle density matrix of the ^{3}He atoms ($N_3=38$ $N_4=49$, $x=44\%$). Solid curve—^{3}He atoms, dot-dashed curve—ideal Fermi gas, solid circles—see text.

1. Single-particle density matrices, the condensate fraction, and the momentum distributions

The smoothed values of the single-particle density matrices $\rho_1^4(r)$ and $\rho_1^3(r)$ are plotted in Figs. 2 and 3, respectively. For both functions the scatter of the original data from the smoothed curve is typically 0.01 in the region $r > \sigma$ and almost always less than 0.02. For the region $\sigma > r > 0.3\sigma$ the scatter increases from 0.02 to about 0.05. The statistics become poor for $r < 0.3\sigma$ so that the smoothed values which we have shown by solid circles, are unreliable. This can be seen also from the fact $\rho_1^4(r)$ does not approach unity as it should. Therefore, we have replaced the calculated values of $\rho_1^\alpha(r)$ in the region $0 \leq r \leq 0.27\sigma$ by a parabolic interpolation between $\rho_1^\alpha(0)=1$ and $\rho_1^\alpha(0.27\sigma)$, $\alpha=3$ or 4. The interpolations are represented by the dashed curves in Figs. 2 and 3. Using these interpolations should give a more reasonable large-k behavior of the momentum distribution $N^\alpha(k)$, which is obtained by Fourier transforming $\rho_1^\alpha(r)$, than using the computed values directly. The functional form of $\rho_1^\alpha(r)$ for small r is not known. However, the slope of $\rho_1^\alpha(r)$ at $r=0$ must be zero, because, otherwise, the cusp at $r=0$ which behaves like $e^{-\eta r}$ would give an asymptotic momentum distribution like $(k^2+\eta^2)^{-2}$, for which the kinetic energy $\int N^\alpha(k)k^2\,d^3k$ diverges. Our parabolic interpolation is a simple choice which satisfies this requirement.

a. ^{4}He component condensate fraction. In Fig. 2, the limiting value of $\rho_1^4(r)/\rho_4$ for large r gives a condensate fraction of $19\pm1\%$. The condensate fraction n_0 of the solution is larger than that of pure ^{4}He, which is about 12% for $b=1.16$ and $\rho=\rho_0$.[26] This enhancement seems to be due to the fact that the average density of the solution is smaller than that of pure ^{4}He, and hence the probability of atoms being scattered out of the condensate is less. To verify this, we have done a calculation in which exactly the same parameter ($b=1.145$) as in the (14,18) calculation was used except that the determinants were deleted from the wave function. This can be viewed as a solution of mass-3 bosons and mass-4 bosons. The ^{4}He condensate fraction so obtained is $18\pm1\%$ which is very close to the fermion-boson solution. Thus the Fermi statistics of the ^{3}He atoms do not play an important role in determining n_0. Notice in Table I that, for a given concentration, n_0 is not sensitive to the number of particles used in the period cell.

b. ^{3}He component. The single-particle density matrix for ^{3}He atoms $\rho_1^3(r)$, which is shown in Fig. 3, becomes negative at $r_0\approx2.76\sigma$, in contrast to the fact that $\rho_1^4(r)$ is always positive.

For noninteracting ^{3}He atoms, the angular averaged single-particle density matrix $\rho_1^{(0)}(r)$ can be calculated analytically to be

$$\frac{\rho_1^{(0)}(r)}{\rho_3}=\frac{1}{I}\sum_{k\leq k_F}\frac{\sin kr}{kr}=\begin{cases}\frac{1}{7}\left[1+\frac{3L_7}{\pi r}\sin\frac{2\pi r}{L_7}\right], & I=7\\ \frac{1}{19}\left[1+\frac{3L_{19}}{\pi r}\left(\sin\frac{2\pi r}{L_{19}}+\sqrt{2}\sin\frac{2\sqrt{2}\pi r}{L_{19}}\right)\right], & I=19\\ \frac{1}{27}\left[1+\frac{3L_{27}}{\pi r}\left(\sin\frac{2\pi r}{L_{27}}+\sqrt{2}\sin\frac{2\sqrt{2}\pi r}{L_{27}}+\frac{4}{3\sqrt{3}}\sin\frac{2\sqrt{3}\pi r}{L_{27}}\right)\right], & I=27\end{cases}, \tag{20}$$

where $k_F=(3\pi^2N_3)^{1/3}/L_l$ and L_l is determined for each value of $N(=N_3+N_4)$ according to Eq. (4). This means that

$$k_F=(3\pi^2x/v_4)^{1/3}/(1+\alpha x)^{1/3} \ .$$

The subscripts on L are a reminder that x varies slightly with N_3 for integral values of N_3 and N_4. In Eq. (20) the x values are close to 44%. The values $I=7$, 19, and 27 are the three smallest numbers of fermions which can occupy the Fermi sphere symmetrically. These functions are all represented by the single dot-dashed curve in Fig. 3, because their values are very close in the range $r<3.2\sigma$ of the figure. For an infinite ideal Fermi gas system the single-particle density matrix is

$$\frac{3(\sin k_Fr-k_Fr\cos k_Fr)}{(k_Fr)^3} \ .$$

The values of this function for $r<3.2\sigma$ are also very close to those of Eq. (20). For $r>3.2\sigma$ the curves would differ appreciably.

c. Momentum distributions. The momentum distribution of the ^{4}He atoms, given by

$$N^4(k)=\int d^3r\, e^{i\vec{k}\cdot\vec{r}}[\rho_1^4(r)-n_0] \ , \qquad (21)$$

is shown in Fig. 4. The single-particle density matrix $\rho_1^4(r)$ used for this calculation is based on the smoothed data in Fig. 2 for $r>0.27\sigma$ and by the parabolic interpolation mentioned above for $r<0.27\sigma$. The values of $N^4(k)$ for $k>5\sigma^{-1}$ should not be considered to be reliable because of the more limited data on $\rho_1^4(r)$ for small r. A clear indication of this is that $N^4(k)$ (with $x=44\%$) becomes negative at $k=11.2\sigma^{-1}$. The values of $N^4(k)$ are not reliable for small k where they depend on the asymptotic behavior of the difference $\rho_1^4(r)-n_0$, which should be like r^{-2} since it is believed that $N^4(k)$ is proportional to k^{-1} at small k.[27] Therefore, the curves in Fig. 4 are probably reliable in the interval $1\sigma^{-1}<k<5\sigma^{-1}$.

For the ^{3}He atoms $\rho_1^3(r)$ presumably has long-range oscillations which are important in determining the discontinuity of $N^3(k)$ at the Fermi momentum. We have only the values of $\rho_1^3(k)$ for $r<3.2\sigma$ (containing less than one cycle of the oscillation), which is not enough to allow a reliable calculation of $N^3(k)$. Nevertheless, the fact that the two curves cross the abscissa at nearly the same point suggests that we can estimate a rough upper bound to the discontinuity ΔN in $N^3(k)$ at k_F. We assume that $N^3(k)$ has a step ΔN and a smooth broad background just as in the calculations by Ceperley *et al.*[19] [see their Fig. 2(d)]. Then $\rho_1^3(r)$ will be $\Delta N\rho_1^{(0)}(r)$ plus a short-range part which is already negligible before the first crossing. Therefore, the ratio $\rho_1^3(r)/\rho_1^{(0)}(r)$ near the common crossing give an estimate of ΔN. Applied to Fig. 3(c) of Ref. 19, this gives $\Delta N\sim0.4$ for $x=1$, which is consistent with their Fig. 2(d). In our case Fig. 3 permits only very rough estimate $\Delta N<0.2$ for $x=0.44$.

2. *Radial distribution functions (RDF) and the structure factors*

The smoothed values of the RDF's $g_p(r)$, $g_a(r)$, and their sum, which is $g_{33}(r)$, are plotted in Fig. 5. The Pauli hole effect seems to dominate the variation of $g_p(r)$ outside the repulsive core region and the peak at the first coordination shell, which appears in $g_a(r)$, is absent. A similar peakless variation of $g_p(r)$ characterizes the calculations of pure ^{3}He by Ceperley

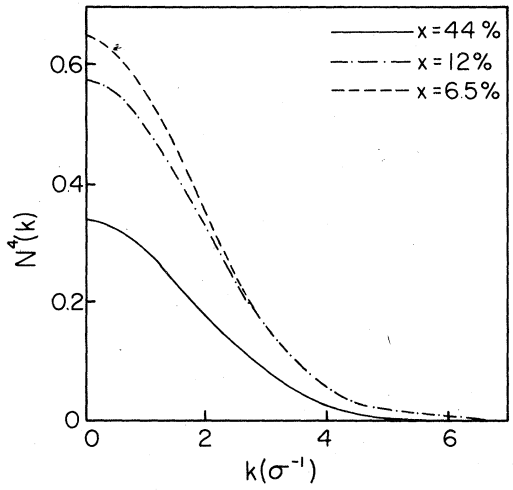

FIG. 4. Momentum distribution $N^4(k)$.

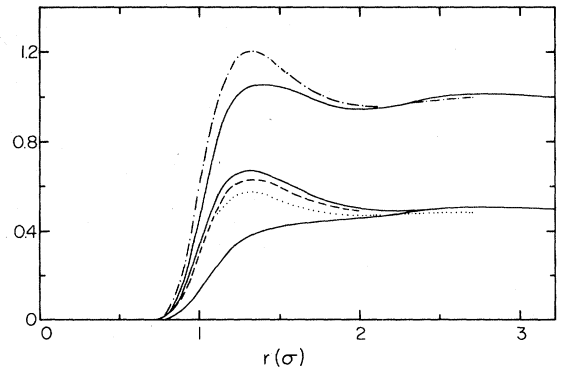

FIG. 5. Radial distribution functions ($N_3=38$, $N_4=49$, $x=44\%$). Solid curves: upper$-g_{33}(r)$, middle$-g_a(r)$, lower$-g_p(r)$. Broken curves: dot-dashed$-g_{33}'(r)$, dashed$-g_a'(r)$, dotted$-g_p'(r)$.

et al.[19] The Pauli hole can be removed by dropping the determinant factors $d_\uparrow, d_\downarrow$ from $\psi(\vec{r}_1, \ldots, \vec{r}_{N_3}; \vec{r}_{N_3+1}, \ldots, \vec{r}_N)$ in Eq. (3). The radial distribution functions $g_p'(r)$ and $g_a'(r)$ so obtained are shown by the dotted and dashed curves, respectively, in Fig. 5 along with their sum $g_{33}'(r)$ which is shown as the dot-dashed curve. [We have calculated $g_p'(r)$ and $g_a'(r)$ only up to $r=2.71\sigma$]. The fact that $g_p'(r)$ is closer to $g_a(r)$ than to $g_p(r)$ confirms the role of the Pauli hole in determining the shape of the latter.

The values of $g_a(r)$ are higher than those of $g_a'(r)$ in the region of the first maximum because the Pauli hole reduction of the number of atoms of parallel spin in that region, where the potential is attractive, permits more atoms of antiparallel spin to move in. If the system were of infinite size $g_p'(r)$ and $g_a'(r)$ would be identical because there is no longer any distinction in ψ between up- and down-spin particles. However, for a fixed number of particles of each label $3\uparrow$ or $3\downarrow$ in the volume Ω, the functions g and g' satisfy the integral relation,[28]

$$\int_\Omega [g_x(\vec{r}) - \tfrac{1}{2}]\, d^3r = \begin{cases} -\rho_3^{-1}, & x = p \\ 0, & x = a \end{cases}, \qquad (22)$$

which expresses the fact that, if α is the label of the atom at the origin, there are only $N_\alpha - 1$ atoms of that label remaining in Ω. For the Slater-Jastrow ψ the Pauli hole excludes precisely one particle of parallel spin so that g_p can go strictly to the value $\frac{1}{2}$ at large enough distances. The situation is different for the primed g's where the deficit $-\rho_3^{-1}$ in Eq. (22) for g_p' requires a small reduction in the uniform density at large distances to compensate for the filling in of the Pauli hole. If we assume that $\Delta g' \equiv g_a' - g_p'$ is constant throughout most of Ω, then $\Delta g' \cong N_3^{-1} \simeq 0.026$, which is consistent with our data as shown in Fig. 5 at large distances.

The RDF's $g_{34}(r)$ and $g_{44}(r)$ are plotted in Fig. 6.

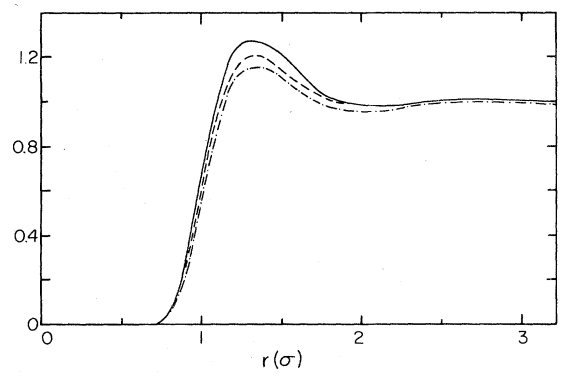

FIG. 6. Radial distribution functions ($N_3=38$, $N_4=49$, $x=44\%$). Solid curve$-g_{34}(r)$, dot-dashed curve$-g_{44}(r)$, dashed curve$-g_{34}'(r)$.

Notice that the value of the first maximum of $g_{34}(r)$ is larger than that of $g_{44}(r)$. Similar to the differences between $g_a(r)$ and $g_a'(r)$, this difference between $g_{34}(r)$ and $g_{44}(r)$ is due to the fact that the Pauli hole forces the ^{3}He atoms with parallel spins to spend more time around the ^{4}He atoms.

Let $g_{\alpha\beta}'(r)$, $\alpha, \beta = 3$ or 4 denote the RDF's corresponding to $g_{\alpha\beta}(r)$, except that $g_{\alpha\beta}'(r)$ are obtained from the calculation in which the determinants are deleted from the wave function. The dashed line in Fig. 6 represents $g_{34}'(r)$. For $r < 1.75\sigma$, there are no statistically significant differences between the values of $g_{34}'(r)$, $g_{33}'(r)$, and $g_{44}'(r)$. For $r > 1.7\sigma$, however, the values of $g_{33}'(r)$ and $g_{44}'(r)$ (not shown in Fig. 6) are consistently lower than those of $g_{34}'(r)$ by about 0.02 again because of the difference in the normalizations: as defined by Eq. (22) with $\frac{1}{2}$ and ρ_3^{-1} replaced by 1 and $\rho_\alpha^{-1}\delta_{\alpha\beta}$, respectively. The lowering of $g_{44}'(r)$ is slightly smaller than that of $g_p'(r)$ because $N_4 > N_3$.

For an appreciation of the statistical uncertainties we give the comparison between the computed RDF's and the smoothed RDF's as follows: From $r=0.75\sigma$ to 1.2σ the scatter of the original data points from the smoothed curves varies from 0.01 to 0.05. However, because of the sharp rise of these functions in this region, we can still draw rather smooth curves thorugh the original data points. Around the first maximum, between say, $r=1.2\sigma$ and 1.9σ, the scatter of the data points from the smoothed curves is typically 0.02. For $r > 1.9\sigma$, the scatter is typically 0.01 or less.

The structure factors $S_{34}(k)$ and $S_{44}(k)$ are plotted in Fig. 7, while $S_p(k)$, $S_a(k)$, and $S_{33}(k)$ are

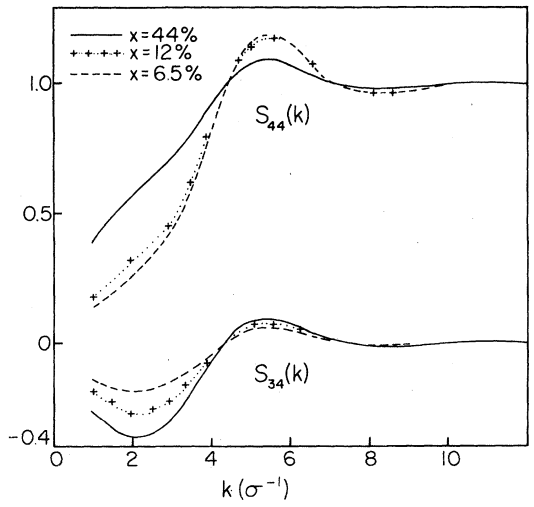

FIG. 7. Structure factors. The upper curves are $S_{44}(k)$ while the lower curves are $S_{34}(k)$. The solid lines are for $x=44\%$, the dashed for $x=12\%$ and the crosses plus dots for $x=6.5\%$.

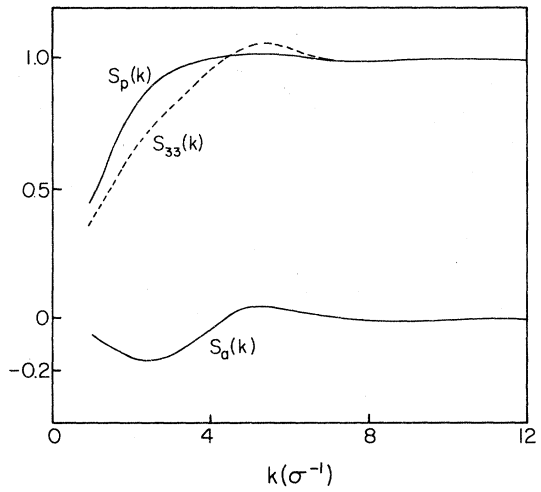

FIG. 8. Structure factors $S_p(k)$, $S_a(k)$, and $S_{33}(k)$ ($N_3=38$, $N_4=49$, $x=44\%$).

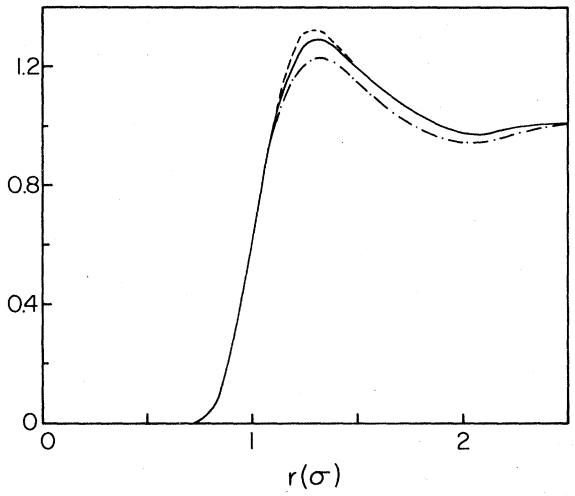

FIG. 9. Radial distribution functions $g_{34}(r)$ and $g_{44}(r)$ for 6.5% and 12% solutions. The solid curve is $g_{34}(r)$ for $x=12\%$; the dashed curve is $g_{34}(r)$ for $x=6.5\%$; and the dot-dashed curve is $g_{44}(r)$ for both $x=6.5\%$ and 12%.

plotted in Fig. 8. They are obtained by using Eq. (18). The difference between the values of the structure factors obtained by the smoothed RDF's and those obtained by the unsmoothed RDF's are typically 0.003 to 0.002 for $0 < k \leq 1\sigma^{-1}$, and always less than 0.001 for $k > 1\sigma^{-1}$. Owing to the lack of detailed information about the RDF's for $r > 3.2\sigma$, the values of the structure factors for $k < 1\sigma^{-1}$ are not reliable and, therefore, are not shown in the figures. According to the theory of Tan *et al.*,[29] which is based on the compressibility sum rule, $S_{\alpha\beta}(k)$ should be proportional to k for small k.

B. 12% and 6.5% Solutions

The 12% and the 6.5% solutions were simulated by doing (14,100) ($x=12.28\%$) and (14,201) ($x=6.51\%$) calculations. Owing to the fact that the minimum of E in the (14,18) calculation (Fig. 1) is shallow and that the optimal value of the parameter b, namely, $b=1.145$, is rather close to the optimal value 1.16 for pure liquid ^{4}He, we expect that the optimal value of b for these rather dilute solutions should not be very different from that of pure ^{4}He. Therefore, we have taken $b=1.16$ for the (14,100) and the (14,201) calculations. The values of the average binding energy and the condensate fractions are given in Table I. The statistical uncertainties in E_3, T_3, and F_3^2 are larger than those of the (14,18) calculation. The reason is that, even though about the same number of moves are generated for all the calculations, the data samples collected for the quantities E_3, T_3, and F_3^2 which pertain to ^{3}He are smaller. For the same reason the statistics are not good enough to allow reliable calculation of the RDF's $g_p(r)$, $g_a(r)$, and the single-particle density matrix $\rho_1^3(r)$ for the ^{3}He atoms.

The $\rho_1^4(r)$ obtained in the (14,100) ($x=12\%$) calculation and that obtained by a (0,32) calculation (that is for pure liquid ^{4}He) are plotted in Fig. 2.

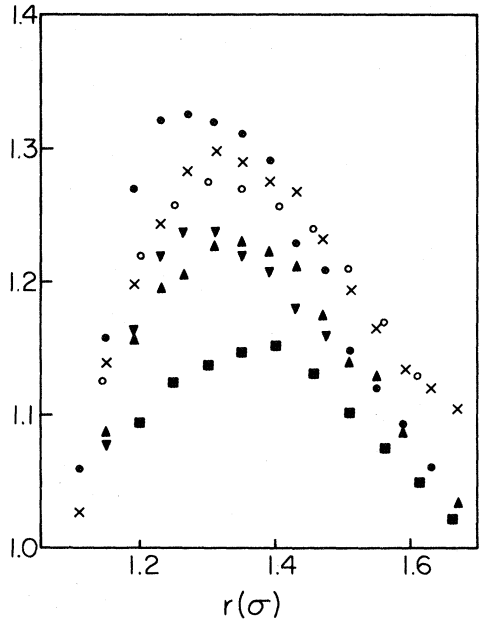

FIG. 10. Radial distribution functions near the first maxima. ●—$g_{34}(r)$, $x=6.5\%$, ▼—$g_{44}(r)$, $x=6.5\%$; ×—$g_{34}(r)$, $x=12\%$, ▲—$g_{44}(r)$, $x=12\%$, ○—$g_{34}(r)$, $x=44\%$; ■—$g_{44}(r)$, $x=44\%$.

The values of $\rho_1^4(r)$ obtained in the (14,201) ($x=6.5\%$) calculation lie between those of the (14,100) and (0,32) calculations. Similar to the calculation for the 44% solution, we have replaced the computed values of $\rho_1^4(r)$ in the region $0 < r \leq 0.27\sigma$ by a parabolic interpolation between $\rho_1^4(0)=1$ and $\rho_1^4(0.27\sigma)$.

The momentum distribution $N^4(k)$ obtained by Eq. (21) for the (14,100) and the (14,201) calculations are plotted in Fig. 4. The values of the condensate fraction for these calculations are given in Table I.

The results of $g_{34}(r)$ and $g_{44}(r)$ for the (14,100) and the (14,201) calculations are shown in Fig. 9. The first maximum of $g_{34}(r)$ is again larger than that of $g_{44}(r)$, that is, the effect of the Pauli hole can still be seen in these relatively dilute solutions. As the ^{3}He concentration increases, the positions of the first maximum of $g_{34}(r)$ and $g_{44}(r)$ shift to the larger r values, while the values of the maximum decrease. This behavior is displayed in Fig. 10 and is attributable to the combined effect of the decrease in the average total density and partial density of ^{4}He as the ^{3}He concentration increases. The structure factors are plotted in Fig. 7.

IV. DISCUSSION

In Table I we see that the calculated average binding energy per atom for the 6.5% solution is -5.45 K as compared to the experimental value of -6.87 K found by Seligmann *et al.*[30] This is not surprising because the variational calculation gives the upper bound of the ground-state energy. For bulk liquid ^{4}He the upper bound of the ground-state energy found by Schiff and Verlet[5] was -5.95 K as compared to the experimental values of -7.14 K. The comparison with experiment for $x > 6.5\%$ is not possible because of phase separation in the real solutions at those concentrations.

We believe that the enhancement of the condensate fraction in the 44% solution can be experimentally observable for the following reasons: Dokukin *et al.*[15] and also Sears and Svensson[16] have measured the condensate fraction in pure liquid ^{4}He over a considerable range of the temperature, and they fit their results approximately to the dependence given in Eq. (2). If similar behavior exists in the 44% solution,[31] one should be able to observe n_0 at a temperature 0.75 K. Just above this temperature the real 44% solution is stable with $T_\lambda = 1.4$ K. Using Eq. (2) we find that $n_0(T=0.75\text{ K}) = 0.97 n_0(0)$. This suggests that an inelastic neutron scattering experiment on a solution of this ^{3}He concentration and at a temperature slightly above 0.75 K may see the enhancement of the condensate fraction.

We have found that, for a given ^{3}He concentration, the value of the first maximum of $g_{34}(r)$ is larger than that of $g_{44}(r)$. This behavior exists for all the concentrations used in our calculations. This phenomenon in the 6.5% solution should be observable at low enough temperatures, say less than 0.02 K, at which the ^{3}He atoms become a degenerate Fermi liquid. We expect these properties to be less profound experimentally in the 12% and 44% solutions just above the phase separation line because the fermions are not fully degenerate. From the relation $T_F(x) = \hbar^2 k_F^2 / 2 m_3^* k_B$ for the degenerate temperature and the approximate constancy of m_3^* with x, $m_3^* \simeq 3 m_3$, we estimate $T_F(0.12) = 0.48$ K and $T_F(0.44) = 1.14$ K as compared with the phase separation temperature of 0.2 and 0.75 K, respectively. It should be pointed out that this behavior of $g_{34}(r)$ and $g_{44}(r)$ is based on the use of the same Jastrow factors $u(r)$ for all the species [Eq. (5)], and the basis for it seems to be the Pauli exclusion principle. The use of species-dependent Jastrow factors is not expected to change this behavior and the cost of optimizing such a more complex wave function did not appear to be justified.

Some comments are worth making on the relationship to recent work, some of which has appeared since this manuscript was submitted. Guyer and Miller[32] have analyzed the conditions of miscibility of isotopic fermion-boson mixtures in the ground state using the Slater-Jastrow function, Eq. (3), as starting point but making the lowest-order fermion cluster approximation for the pair correlation functions $g_{\alpha\beta}$ which are implicit in the terms in Eq. (7) for the total ground-state energy. For example, they use $g_{34} = g_{44}$, whereas Fig. 6 shows a significant difference as mentioned above. Their quantitative conclusions should change somewhat as they themselves have already estimated by estimating the effect of including three-body exchange. Our work has not been directly concerned with miscibility and there is no evidence of phase separation in the Monte Carlo runs. This may be due in part to the periodic boundary conditions and small particle numbers and may provide a way to calculate the homogeneous phase $E(x)$ needed in their analyses.

Owen[33] has discussed the optimization of the Slater-Jastrow wave function for pure ^{3}He both by improving the form of $u(r)$ at intermediate and large r through incorporation of virtual excitations of the fermions and through assuming a state dependence, $u_p(r)$. The linear dependence of $S(k)$ on k at small k is obtained, which is not accessible in the present calculations nor those of Ref. 19.

ACKNOWLEDGMENTS

One of us (W.-K.L.) would like to thank the Research Council of the University of Cincinnati for support during part of this work. We thank Dr. Aneesur Rahman for his help.

*Present address: Dept. of Physics, Purdue University, W. Lafayette, Ind. 47907.

[1]J. Bardeen, G. Baym, and D. Pines, Phys. Rev. 156, 207 (1966); V. J. Emery, *ibid.* 161, 194 (1967); C.-W. Woo, H. T. Tan, and W. E. Massey, *ibid.* 185, 287 (1969), and the references therein.

[2]J. C. Owen (unpublished) has shown that the Feynman-Cohen backflow wave function gives $m_3^* = 1.6 - 1.7 m_3$ compared with the experimental value of $2.3 m_3$.

[3]O. Penrose and L. Onsager, Phys. Rev. 104, 576 (1956).

[4]W. L. McMillan, Phys. Rev. 138, A442 (1965).

[5]D. Schiff and L. Verlet, Phys. Rev. 160, 208 (1967).

[6]W. P. Francis, G. V. Chester, and L. Reatto, Phys. Rev. A 1, 86 (1970).

[7]P. M. Lam and C. C. Chang, Phys. Lett. 59A, 356 (1976).

[8]L. Reatto, Phys. Rev. 183, 334 (1969).

[9]P. A. Whitlock, D. M. Ceperley, G. V. Chester, and M. H. Kalos, Phys. Rev. B 19, 5598 (1979).

[10]G. V. Chester, in *The Helium Liquids,* edited by J. G. M. Armitage and I. E. Farquhar (Academic, New York, 1975), p. 1.

[11]P. C. Hohenberg and P. M. Platzman, Phys. Rev. 152, 198 (1966).

[12]H. A. Mook, R. Scherm, and M. K. Wilkinson, Phys. Rev. A 6, 2268 (1972); L. J. Rodriguez, H. A. Gersch, and H. A. Mook, Phys. Rev. A 9, 2085 (1974); H. W. Jackson, Phys. Rev. A 10, 278 (1974); H. A. Mook, Phys. Rev. Lett. 32, 1167 (1974); L. Aleksandrov, V. A. Zagrebnov, Zh. A. Kozlov, V. A. Parfenov, and V. B. Priezzhev, Sov. Phys. JETP 41, 915 (1975) [Zh. Eksp. Teor. Fiz. 68, 1825 (1975)].

[13]O. K. Harling, Phys. Rev. A 3, 1073 (1971).

[14]A. D. B. Woods and V. Sears, Phys. Rev. Lett. 39, 415 (1977).

[15]E. B. Dokukin, Zh. A. Kozlov, V. A. Parfenov, and A. V. Puchkov, JETP Lett. 23, 453 (1976) [Pis'ma Zh. Eksp. Teor. Fiz. 23, 497 (1976)].

[16]V. F. Sears and E. C. Svensson, Phys. Rev. Lett. 43, 2009 (1979); similar measurements but over a more limited temperature have been done by H. D. Robkoff, D. A. Ewen, and R. B. Hallock, *ibid.*, p. 2006.

[17]F. W. Cummings, G. J. Hyland, and G. Rowlands, Phys. Konden. Mater. 12, 90 (1970).

[18]The interpretation of the temperature dependence of the pair correlation function in terms of $n_0(T)$ according to the Cummings, Hyland, and Rowlands prescription remains controversial and its assumptions have been criticized by A. Griffin, Phys. Rev. B 22, 5193 (1980), and by G. Chester and L. Reatto, *ibid.*, p. 5199, and by A. L. Fetter, *ibid.* 23, 2425 (1981). An apparently different interpretation in terms of roton contributions to the structure factor has been proposed by C. DeMichelis, G. L. Masserini, and L. Reatto, Phys. Lett. 66A, 484 (1978), and G. Gaglione, G. L. Masserini, and L. Reatto, Phys. Rev. B 22, 1237 (1980).

[19]D. Ceperley, G. V. Chester, and M. H. Kalos, Phys. Rev. B 16, 3081 (1977).

[20]J. Wheatley, Am. J. Phys. 36, 18 (1968).

[21]D. O. Edwards, E. M. Ifft, and R. E. Sarwinski, Phys. Rev. 177, 380 (1969).

[22]Before 1976, all the Monte Carlo and molecular dynamics calculations for liquid ^{4}He minimize $E_4' = T_4' + V_4$. Here we minimize E in Eq. (6) rather than $E' = x(T_3' + V_3) + (1-x)(T_4' + V_4)$ because the statistical uncertainty of E is roughly half of that of E'. This fact has been found independently by Ceperley *et al.* (Ref. 19) and has been attributed (private communication from C. E. Campbell) to the fact that the integrand of E is an approximation to $\Psi_0 H \Psi_0 = \text{const} \Psi_0^2$ (where const $= E_0$, the exact ground-state energy) while the integrand of E' is not an approximation to $\Psi_0 H \Psi_0$.

[23]W. L. McMillan (private communication).

[24]We found that if $K_D^{(i)} = \sum_{j=1}^{N} \bar{D}_{ji}^s \nabla_i^2 \phi_j(r_i)$ is calculated *after each move* and take the average over all the moves, we get a value which is very close to the analytical result with a remarkably small fluctuation of 0.001 which is much smaller than the fluctuations in other quantities. This provides an incidental test of the simplified Monte Carlo sampling procedure due to McMillan (Ref. 3).

[25]Our computer program was set up in such a way that only pairs with distance less than $L/2$ can be taken into account. There is no difficulty in setting up a computer program to calculate the pair functions with separation larger than $L/2$. This, however, might give rise to undesirable artifacts because of the use of periodic boundary conditions.

[26]The value is somewhat larger than the 11% obtained by McMillan and also Schiff and Verlet because they have used $b = 1.17$.

[27]J. Gavoret and P. Noziéres, Ann. Phys. (N.Y.) 28, 349 (1964).

[28]See, for example, E. Feenberg, *Theory of Quantum Fluids* (Academic, New York, 1969), Chap. 1.

[29]H. T. Tan, C. -W. Woo, and F. Y. Wu, J. Low Temp. Phys. 4, 261 (1971).

[30]P. Seligmann, D. O. Edwards, R. E. Sarwinski, and J. T. Tough, Phys. Rev. 181, 415 (1969).

[31]It is interesting that the experimental results of Tominaga *et al.* [J. Phys. C 8, 420 (1975)] show that the *superfluid density* in ^{3}He-^{4}He solutions have the same temperature dependence as that in pure liquid ^{4}He. So, it seems not unreasonable to conjecture that the condensate fraction of the solution has the same temperature dependence as that of pure liquid ^{4}He.

[32]R. D. Guyer and M. D. Miller, Phys. Rev. B 22, 142 (1980).

[33]J. C. Owen, Phys. Rev. B 23, 2169 (1981), and Phys. Lett. 89B, 303 (1980).